Nuclear Stopping: Paving the way from RHIC to LHC

Hans Hjersing Dalsgaard[*]

for the BRAHMS collaboration

Nuclear stopping has been measured at a range of different energies in heavy ion experiments. In this contribution proton data from the BRAHMS experiment at RHIC running at $\sqrt{s_{NN}} = 62.4 GeV$ are presented. Furthermore data from AGS, SPS and RHIC are used to estimate the stopping, energy loss and multiplicity at LHC.

1. Nuclear Stopping and Energy Loss

The stopping is quantified as the average rapidity loss[1]. It is defined as (assuming a collider experiment):

$$\delta y = y_{beam} - \frac{2}{N_{part}} \int_0^{y_{beam}} y \frac{dN_{B-\bar{B}(y)}}{dy} dy \qquad (1)$$

Here N_{part} is the number of participant nucleons in the collision, y_{beam} is the beam rapidity and $\frac{dN_{B-\bar{B}(y)}}{dy}$ is the net-baryon rapidity density. For a collider setup the energy loss is subsequently defined as:

$$\delta E = E_{beam} - \frac{2}{N_{part}} \int_0^{y_{beam}} m_T \cosh y \frac{dN_{B-\bar{B}(y)}}{dy} dy \qquad (2)$$

Here E_{beam} is the beam energy.

2. The BRAHMS Experiment

In Fig. 1 is shown a sketch of the BRAHMS experiment[2]. It consists of two spectrometers: *The Midrapidity Spectrometer*, MRS and *The Forward Spectrometer*. Together the spectrometers enable detection of (anti)protons within the range $-0.1 < y < 3$. BRAHMS use a set of global detectors to determine centrality and vertex. See the BRAHMS NIM report[3] for a full description of the experimental setup. In this analysis only events in the centrality class 0-10 % have been included. Tracking is provided by two Time Projection Chambers (TPC) in the MRS and

[*]Niels Bohr Institute, University of Copenhagen, Blegdamsvej 17, 2100 Copenhagen, Denmark

2   *Hans Hjersing Dalsgaard (Nuclear Stopping: Paving the way from RHIC to LHC)*
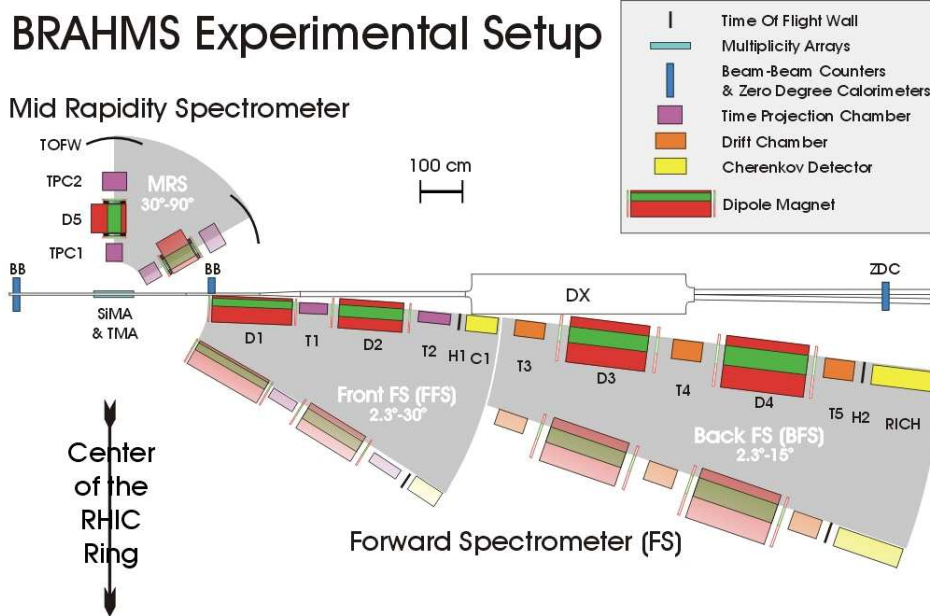

Fig. 1. The BRAMHS experiment at RHIC.

two TPCs and three Drift Chambers in the FS. Particle IDentification (PID) is done using Time Of Flight and Ring Imaging CHerenkov detectors. The data have been corrected for geometrical acceptance, tracking efficiency, PID efficiency, absorption and multiple scattering. These corrections are based on simulations using GEANT[4].

3. Spectra and Yields

In Fig. 2 the p_T spectra, $\frac{1}{2\pi p_T}\frac{d^2N}{dydp_T}$ from the analysis are shown. The spectra have been fitted to a Gaussian in p_T:

$$f(p_T) \propto e^{\frac{-p_T^2}{2\sigma^2}} \tag{3}$$

The rapidity densities, $\frac{dN}{dy}$ are obtained from the integral of the fit function and thus corresponds to an extrapolation of the data into the full p_T range.

The systematic error on $\frac{dN}{dy}$ has been estimated by varying the binwidth, fitrange and fit function. These systematic errors are less than 10 % at all settings except at $y \sim 2.5$ where it is $\sim 15\%$.

4. Rapidity Losses

An estimate for the net-baryon $\frac{dN_{B-\bar{B}(y)}}{dy}$ rapidity loss can be derived from the measured $\frac{dN}{dy}$ for protons. Using a similar procedure as in a previous BRAHMS
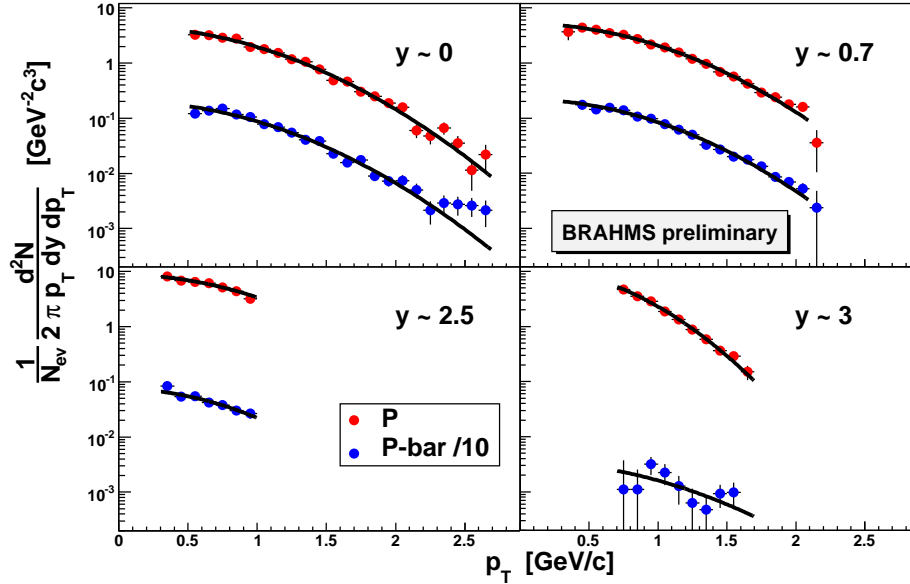
Fig. 2. (anti)Proton p_T spectra fitted with Gaussians in p_T

publication on stopping[5] the conversion $N_b = 2 \cdot N_p$ was used. For the centrality class 0-10 % $N_{part} = 314 \pm 6$ was found from Glauber calculations. This is important as baryon conservation constrains the integral of $\frac{dN_{B-\bar{B}(y)}}{dy}$ to $N_b = N_{part}$. This is equivalent to constraining the proton $\frac{dN}{dy}$ to $N_p = N_{part}/2$ which is the procedure used henceforth. In the four upper panels of Fig. 3 $\frac{dN}{dy}$ of protons from AGS (E917[6]), SPS (NA49[9]) and RHIC (BRAHMS[5]) have been plotted together with the results from this analysis. The data has been fitted to a double gaussian in longitudinal momentum, p_z:

$$\frac{dN}{dy} \propto (\exp\left[\frac{-(p_z - \mu)^2}{2\sigma^2}\right] + \exp\left[\frac{-(p_z + \mu)^2}{2\sigma^2}\right]) \tag{4}$$

where the constraint $N_p = N_{part}/2$ has been used for the RHIC data and the constraint $N_p = N_{part}/2.5$ for the AGS and SPS data. The choice of 2.5 is inspired by the approach used by NA49[9]. The rapidity loss from this analysis is 2.16 ± 0.05. The rapidity loss values are also indicated in Fig. 3. Using Eq. 2 the energy loss becomes $\delta E = 25 \pm 1\mathrm{GeV}$.

The bottom panel of Fig. 3 shows the result of a linear extrapolation of the μ and σ values from the fits to the data from the four e lower energies extrapolated to the LHC energy. Taking N_{part} for $\sqrt{s_{NN}} = 5500$ GeV Pb+Pb collisions at LHC to be 380, the rapidity loss and energy loss predicted by this rather bold extrapolation

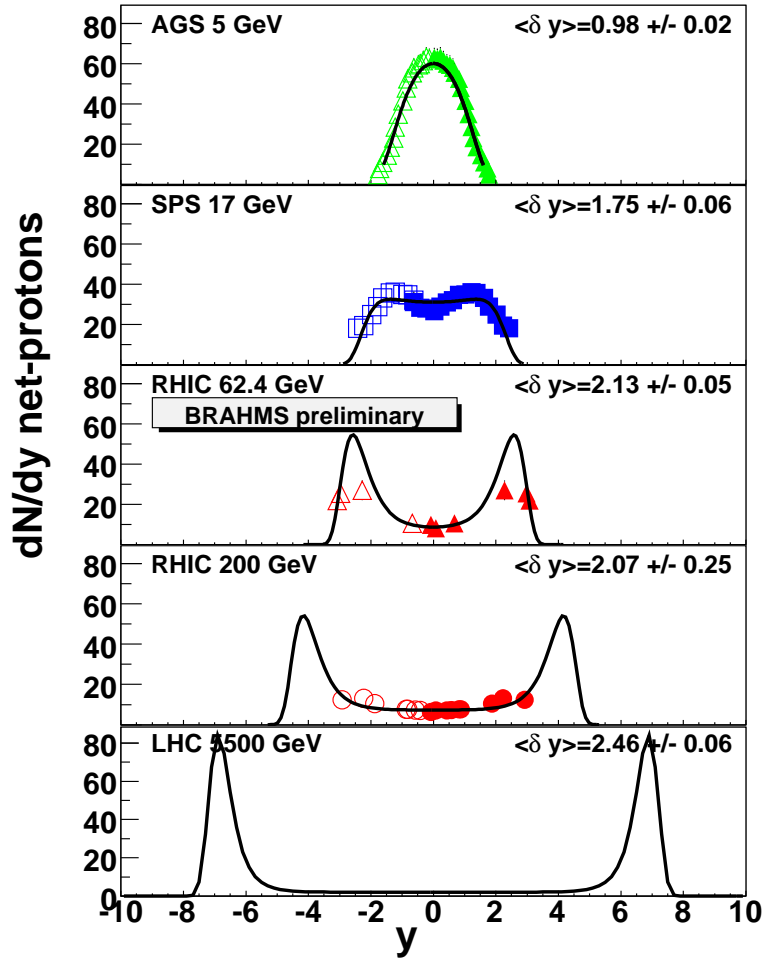4 *Hans Hjersing Dalsgaard (Nuclear Stopping: Paving the way from RHIC to LHC)*

Fig. 3. $\frac{dN}{dy}$ of protons from AGS[6], SPS[9] and RHIC[5]. Errors include systematic errors. Bottom panel shows extrapolation to LHC.

becomes $\delta y = 2.46 \pm 0.1$ and $\delta E = 2290 \pm 60$ GeV, respectively. Thus the amount of the original kinetic energy available for particle production at LHC is expected to be around 80 %. This is about the same amount as for the RHIC top energy[5]. An interesting feature of the extrapolated LHC curve is that is has a non-vanishing midrapidity baryon content. This means that even though the midrapidity baryon content is lower than at RHIC the Bjorken[10] collision scenario is only to some approximation to be expected at LHC. Note that the δy in Fig. 3 are consistent with the values quoted from AGS [6], SPS[9] and RHIC[5] (200 GeV).

5. Systematics of δy

To explore the possible systematics of the rapidity losses found at AGS[6], SPS[9] and RHIC[5] the values are plotted in Fig. 4. The solid curve in Fig. 4 is a fit to the
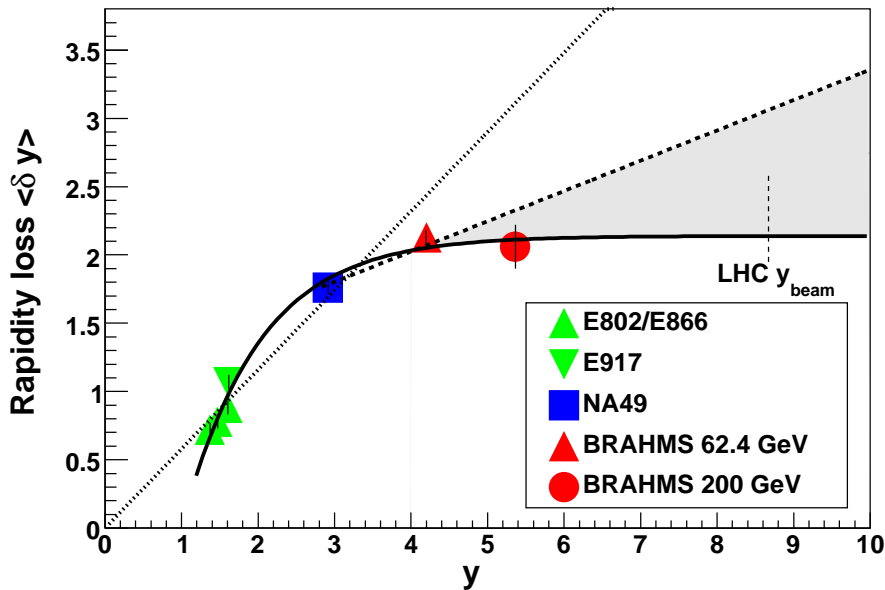

Fig. 4. Rapidity losses from AGS[7,8,6], SPS[9] and RHIC[5] as a function of rapidity. The full drawn line is a fit using Eq. 5 in text. The dashed curve is a straight line fit. Also included as the hashed curve is the linear scaling of δy proposed by Videbaek and Hansen[1].

function:

$$f(y_{CM}) = A + B(1 - \exp(-y_{CM})) \tag{5}$$

This function was selected to reflect the apparent saturating behaviour of the rapidity losses. The dashed line in Fig. 4 is a straight line fit from SPS through RHIC data. Taking these fits as an lower and upper limit for the rapidity loss at higher rapidities, the LHC rapidity loss must be expected to lie somewhere in the range $2.1 < \delta y < 3.4$. It is seen that the result for the rapidity loss at LHC found in Section 4 is consistent with these limits.

Finally, Fig. 4 contains the extrapolation proposed by Videbaek and Hansen[1] that agreed with data up to SPS energies. From Fig. 4 it can be seen that the proposed linear scaling is broken already at $y \approx 4$. Thus the higher energies available at RHIC reveal the onset of a new collision regime, in which the relative stopping $\frac{\delta y}{y_{beam}}$ is decreasing at higher energies.

6. Charged Particle Multiplicity

In Section 4 the energy loss at LHC ($y_{beam} = 8.67$) was predicted to be $\delta E = 2290 \pm 60$ GeV. Assuming that the particle mix has an average m_T of 800 MeV allows an estimate of the charged particle multiplicity given a guess of the shape of the multiplicity distribution. Two cases have been tried in this study: A triangular shape with endpoints at $\pm$LHC y_{beam} and a plateau between rapidities ± 5, dropping linearly off to $\pm$LHC y_{beam}. For these distributions the multiplicities at midrapidity are ~ 3000 and ~ 1300 respectively.

7. Conclusion

The nuclear stopping and energy loss at $\sqrt{s_{NN}} = 62.4$ GeV has been measured and compared to experiments at AGS, SPS and RHIC. This has been used to predict the rapidity and energy loss at LHC as well as derive a $\frac{dN}{dy}$ distribution to be expected for LHC. From this a lower and upper limit for the charged particle multiplicity at midrapidity at LHC has been found.

Acknowledgements

References

1. Videbaek, F. and Hansen, O., Phys. Rev., **C52**, 1995, 2684.
2. Arsene, I. *et al.*, BRAHMS Collaboration, Nucl. Physics, **A757**, 1 (2005).
3. M. Adamczyk *et al.*, BRAHMS Collaboration, Nucl. Instr. and Meth., A499 (2003) 437.
4. GEANT 3.2.1, CERN program library.
5. Bearden, I. G. *et al.*, BRAHMS Collaboration, Phys. Rev. Lett., **93**, 102301 (2004).
6. Back, B. B. *et al.*, E917 Collaboration, Phys. Rev. Lett., **86**, 1970 (2001).
7. E802 Collaboration, L. Ahle *et al.*, Phys. Rev. **60**, 064901 (1999)
8. E877 Collaboration, J. Barette *et al.*, Phys. Rev. **62**, 024901 (2000)
9. H. Appelhauser *et al.*, NA49 Collaboration, Phys. Rev. Lett. **82**, 2471 (1999).
10. J. D. Bjorken, Phys. Rev. D**27**, 140 (1983).